Q:1, 2, 3, 4, 5, 6, 7, 8

Auxin methylation is required for differential growth in *Arabidopsis*

Mohamad Abbas[a,b,1], Jorge Hernández-García[a], Stephan Pollmann[c], Sophia L. Samodelov[d,e], Martina Kolb[f], Jiří Friml[b], Ulrich Z. Hammes[f], Matías Zurbriggen[d], Miguel A. Blázquez[a,2], and David Alabadí[a]

[a]Instituto de Biología Molecular y Celular de Plantas, Universidad Politécnica de Valencia, 46022 Valencia, Spain; [b]Institute of Science and Technology Austria, 3400 Klosterneuburg, Austria; [c]Centro de Biotecnología y Genómica de Plantas, Universidad Politécnica de Madrid–Instituto Nacional de Investigación y Tecnología Agraria y Alimentación, 28223 Pozuelo de Alarcón, Spain; [d]Institute of Synthetic Biology and Cluster of Excellence in Plant Sciences, University of Düsseldorf, 40225 Düsseldorf, Germany; [e]Spemann Graduate School of Biology and Medicine, University of Freiburg, 79085 Freiburg, Germany; and [f]Regensburg University, 93053 Regensburg, Germany

Edited by Ottoline Leyser, University of Cambridge, Cambridge, United Kingdom, and approved May 21, 2018 (received for review April 16, 2018)

Asymmetric auxin distribution is instrumental for the differential growth that causes organ bending on tropic stimuli and curvatures during plant development. Local differences in auxin concentrations are achieved mainly by polarized cellular distribution of PIN auxin transporters, but whether other mechanisms involving auxin homeostasis are also relevant for the formation of auxin gradients is not clear. Here we show that auxin methylation is required for asymmetric auxin distribution across the hypocotyl, particularly during its response to gravity. We found that loss-of-function mutants in *Arabidopsis IAA CARBOXYL METHYLTRANSFERASE1* (*IAMT1*) prematurely unfold the apical hook, and that their hypocotyls are impaired in gravitropic reorientation. This defect is linked to an auxin-dependent increase in *PIN* gene expression, leading to an increased polar auxin transport and lack of asymmetric distribution of PIN3 in the *iamt1* mutant. Gravitropic reorientation in the *iamt1* mutant could be restored with either endodermis-specific expression of *IAMT1* or partial inhibition of polar auxin transport, which also results in normal *PIN* gene expression levels. We propose that IAA methylation is necessary in gravity-sensing cells to restrict polar auxin transport within the range of auxin levels that allow for differential responses.

hormone regulation | auxin metabolism | homeostasis | gravitropism

The plant hormone auxin has long been known to act not only as a key morphogenetic component of differentiation pathways, but also as a coordinator of plant growth in response to environmental stimuli (1, 2). Particularly interesting is the involvement of auxin in the generation of curvatures, such as the apical hook of etiolated seedlings (3, 4), and in the reorientation of organ growth on lateral illumination or in response to gravity (5–7). An essential feature that explains the relevant role of auxin in these processes is the robust mechanism that directs the movement of this hormone through the plant, known as polar auxin transport (PAT) (8–10). Among other consequences, PAT allows the establishment of asymmetric distribution of auxin, which results in differential triggering of auxin responses in different parts of a given organ.

In the case of tropic responses, such as phototropism and gravitropism, it has been estimated that the concentration difference across the hypocotyl may range between 1.5-fold and 2-fold (11–13), similar to the difference in the root tip that triggers gravitropic reorientation (14). The fact that this small difference is sufficient to cause differential growth responses implies that the levels of auxin must be well maintained within a very specific range to ensure that this gradient is informative. Although regulation of the expression, tissue distribution, and cellular localization of the PIN-FORMED (PIN) auxin efflux carriers is presumably the most important mechanism for the maintenance of local auxin maxima (15, 16), it is likely that other mechanisms, such as the regulation of auxin homeostasis, also contribute to this effect (17–19).

Among the pathways that contribute to auxin homeostasis (2), conversion of indole-3-acetic acid (IAA) into methyl-IAA (Me-IAA) by an IAA CARBOXYL METHYLTRANSFERASE (IAMT) could be relevant, because ectopic overexpression of *IAMT1* in *Arabidopsis* disrupts gravitropic responses (20). The specificity of IAMT1 on IAA has been demonstrated for the orthologs in rice and *Arabidopsis* (21, 22). It has been reported that silencing of *IAMT1* in *Arabidopsis* using an RNAi strategy causes a dramatic phenotype that might be explained by simultaneous repression of additional members of the SABATH family (20), which includes methyltransferases for jasmonic acid and other substrates (Fig. 1*A*). Current models consider Me-IAA an inactive form of IAA, because the phenotype caused by *IAMT1* overexpression resembles that of auxin-deficient or auxin-resistant mutants (20), and also because exogenous application of Me-IAA produces the same effects as IAA application (23), which can be explained by hydrolysis of Me-IAA by auxin methyl esterases (24). Given that there is no indication of the physiological relevance of IAA methylation in the generation of differential auxin distribution, we identified and examined the behavior of single *iamt1* loss-of-function mutants under gravistimulation, and found that IAA methylation is required for asymmetric auxin distribution across the hypocotyl.

Results and Discussion

We selected two T-DNA insertion lines (*iamt1-1* and *iamt1-2* in Col-0 and L*er* backgrounds, respectively), the former of which would putatively render a truncated version of IAMT1 lacking

Significance

Auxin is a plant hormone required for the establishment of growth orientation. Redistribution of auxin across an organ allows reorientation, and this is achieved through changes in the polar localization of auxin efflux carriers. We have found that when auxin methylation is impaired, auxin is not correctly redistributed on gravistimulation, due to a general increase in basipetal auxin transport and deficient relocalization of auxin transporters. We conclude that auxin must be within a specific concentration range for its correct distribution, and this range is maintained by auxin methylation in the endodermis, the cell type that perceives gravity.

Author contributions: M.A., J.F., U.Z.H., M.Z., M.A.B., and D.A. designed research; M.A., J.H.-G., S.P., S.L.S., and M.K. performed research; M.A., J.H.-G., S.P., S.L.S., M.K., J.F., U.Z.H., M.Z., M.A.B., and D.A. analyzed data; and M.A.B. wrote the paper.

The authors declare no conflict of interest.

This article is a PNAS Direct Submission.

Published under the PNAS license.

[1]Present address: Plant and Crop Science, University of Nottingham, Loughborough LE12 5RD, United Kingdom.

[2]To whom correspondence should be addressed. Email: mblazquez@ibmcp.upv.es.

This article contains supporting information online at www.pnas.org/lookup/suppl/doi:10.1073/pnas.1806565115/-/DCSupplemental.

PLANT BIOLOGY

PNAS Proof Embargoed

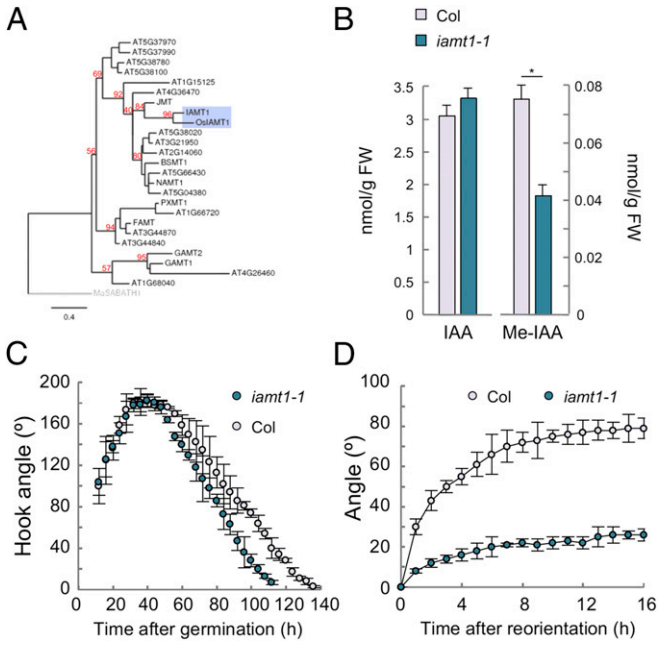


Fig. 1. IAMT1 is necessary for proper differential growth. (*A*) Phylogenetic tree of *Arabidopsis* methyltransferases. Numbers in red represent bootstrap values. (*B*) Levels of IAA and Me-IAA in 3-d-old etiolated seedlings of the *iamt1-1* mutant. Asterisk indicates that the difference is statistically significant (Student's *t* test, $*P < 0.05$). (*C*) Apical hook dynamics in the *iamt1-1* mutant. (*D*) Gravitropic reorientation of *iamt1* mutant hypocotyls.

part of the active site (20) (*SI Appendix*, Fig. S1*A*). Hormone quantification in etiolated seedlings (Fig. 1*B* and *SI Appendix*, Fig. S2*A*) and light-grown seedlings (*SI Appendix*, Fig. S1*B*) showed at least a 50% decrease in the levels of Me-IAA in *iamt1* mutants, confirming in vivo that *IAMT1* encodes an IAA methyltransferase and suggesting that other methyltransferases can also act on IAA or, alternatively, that the truncated proteins encoded by the two *iamt1* alleles might retain some activity. It is also important to note that the decrease in Me-IAA was not accompanied by a significant increase in free IAA levels (Fig. 1*B*), indicating that Me-IAA represents a small proportion in the total IAA pool, in accordance with the observation that *iamt1-1* mutant plants do not display any obvious morphological defects that resemble IAA overaccumulation (*SI Appendix*, Fig. S1*C*).

To investigate if a reduction in IAA methyltransferase activity has an impact in the formation of auxin redistribution, we first examined the dynamics of apical hook development and the hypocotyl response to a gravitropic reorientation, two processes that involve auxin-dependent differential growth (4, 6, 25). The *iamt1* mutants did not display any severe defect in the formation or maintenance of the apical hook, showing only slightly faster opening of the hook (Fig. 1*C* and *SI Appendix*, Fig. S2*B*). In contrast, the ability of the mutant hypocotyls to reorient after gravistimulation was largely impaired (Fig. 1*D* and *SI Appendix*, Fig. S2*C*). Importantly, this different behavior of *iamt1* with respect to the two processes was correlated with the ability of the mutant to redistribute auxin across the hypocotyl in each situation. The asymmetry in the activity of the auxin signaling reporter DR5::GFP across the apical hook was similar in 3-d-old etiolated wild-type (WT) and *iamt1-1* mutant seedlings, despite the higher reporter signal in the mutant (*SI Appendix*, Fig. S3), suggesting no apparent defect in differential auxin distribution during hook formation in etiolated *iamt1-1* seedlings. Nonetheless, the seemingly high auxin signaling in the mutant apical hook might be the cause of its premature opening (Fig. 1*C*). On the other hand, gravistimulation of *iamt1-1* mutant hypocotyls did not provoke the typical accumulation of the DR5 reporter observed on the lower side of WT hypocotyls (6); instead, a similarly high signal was observed on both sides of the mutant hypocotyl before and after the stimulus (Fig. 2 *A* and *B*). This

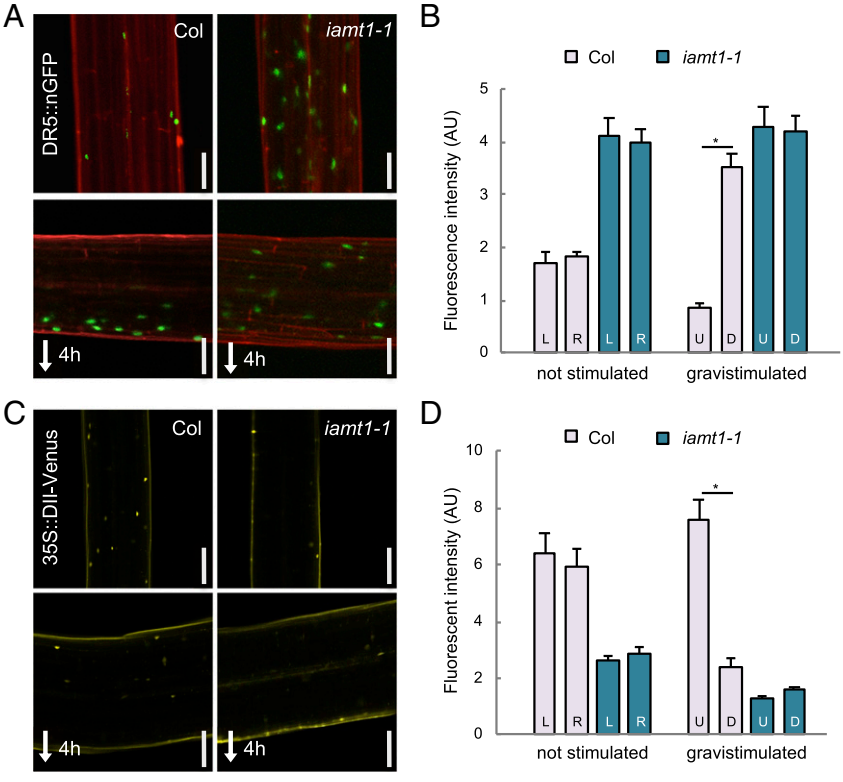


Fig. 2. IAMT1 modulates auxin levels in the hypocotyl. (*A*) DR5::nGFP signal in the hypocotyl of 3-d-old etiolated seedlings before and 4 h after gravistimulation. (*B*) Levels of DR5::nGFP in either side of the hypocotyl. (*C*) DII-Venus signal in the hypocotyl of 3-d-old etiolated seedlings before and 4 h after gravistimulation. (Scale bars: 100 μm.) (*D*) Levels of DII-Venus signal in either side of the hypocotyl. D, down; L, left; R; right; U, up. Asterisks indicate that the difference is statistically significant (Student's *t* test, $*P < 0.001$).

PNAS Embargoed

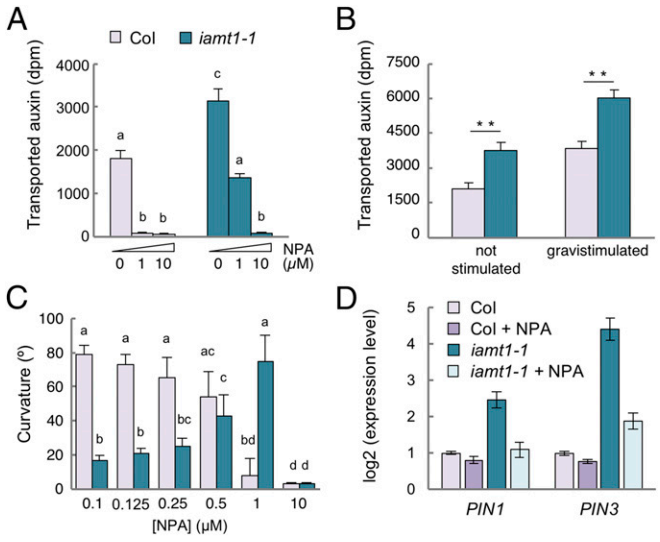


Fig. 3. IAMT1 restricts polar auxin transport in 3-d-old etiolated hypocotyls. (*A*) PAT in unstimulated etiolated hypocotyls. Seedling were treated for 6 h with NPA, followed by a 3-h incubation with [^{3}H]-IAA. (*B*) Effect of 6 h of gravistimulation on PAT in etiolated hypocotyls. (*C*) Effect of NPA on hypocotyl curvature at 12 h after gravitropic reorientation. (*D*) Expression of *PIN1* and *PIN3* in seedlings gravistimulated for 4 h in 0.5 μM NPA or mock solution, determined by qRT-PCR. Values in *A* and *B* are the mean of three biological replicates. In *C*, values are the average of at least 15 seedlings. In all cases, the error bar represents SD. Asterisks indicate that the difference is statistically significant (Student's *t* test, $*P < 0.05$; $**P < 0.01$; $***P < 0.001$). Letters indicate significant differences between groups ($P < 0.05$, one-way ANOVA, Tukey's HSD post hoc test). In *D*, error bars represent SD from three technical replicates. Data from a representative experiment are shown. Two other biological replicates yielded similar results.

defect in the asymmetric auxin response is very likely caused by the inability of the *iamt1-1* mutant to differentially accumulate auxin, as indicated by the loss of signal of a more direct auxin reporter, DII-Venus, on both sides of the hypocotyl (Fig. 2 *C* and *D*).

The findings of no change in the amount of free IAA in whole seedlings in the *iamt1-1* mutant (Fig. 1*B*) and defects in local auxin distribution on gravistimulation (Fig. 2) suggest that alterations in PAT may contribute to the *iamt1* phenotype. In fact, auxin transport along the hypocotyl, measured using ^{3}H-IAA, was nearly twofold higher in the *iamt1-1* mutant compared with the WT (Fig. 3*A*). In both cases, transport was inhibited by incubation with 1-naphthylphthalamic acid (NPA), confirming that enhanced IAA movement was due to increased PAT.

To investigate the observed increase in the IAA transport in *iamt1-1* correlates with the agravitropic phenotype of the mutant, we measured PAT in WT and mutant seedlings with or without gravistimulation. Interestingly, PAT was enhanced in the wild-type and the *iamt1-1* mutant after reorientation (Fig. 3*B*). We next assayed the capacity of WT and mutant seedlings to reorient in the presence of NPA. As expected, the gravitropic reorientation of the hypocotyls of WT seedlings was gradually reduced with increasing doses of NPA (Fig. 3*C*). In contrast, low NPA doses promoted reorientation of *iamt1* seedlings and only a high concentration (10 μM) of NPA abolished it (Fig. 3*C* and *SI Appendix*, Fig. S5*A*). Remarkably, the same amount of NPA restored both the reorientation ability and auxin transport to WT levels in the mutant (Fig. 3 *A* and *C* and *SI Appendix*, Fig. S5*A*). These results suggest a causal connection between the increased PAT in the *iamt1* mutant and its agravitropic phenotype.

The confirmation that a reduction of PAT alleviates the agravitropic phenotype of *iamt1* mutants suggests that PAT restriction by IAA methylation is an important element in asymmetric auxin redistribution. Given that auxin has been proposed to indirectly regulate its own transport (26–28), we hypothesized that the primary effect of the auxin overaccumulation in *iamt1* mutants could in fact be an increase in the expression of *PIN* genes. To test this hypothesis, we measured the transcript levels of *PIN1*, *PIN2*, *PIN3*, and *PIN7* in 3-d-old etiolated seedlings and found at least twofold higher expression levels in *iamt1* mutants (Fig. 3*D* and *SI Appendix*, Figs. S4 and S5*B*). Moreover, transcriptional regulation of *PIN* genes by IAMT1 activity may be physiologically relevant for differential auxin distribution, since gravistimulation provoked not only an increase in PAT in WT seedlings (Fig. 3*B*), but also an increase in the expression of *PIN1* and *PIN3*, albeit with different kinetics (*SI Appendix*, Fig. S4*A*), and, to a lesser extent, of *PIN2* and *PIN7* (*SI Appendix*, Fig. S4*B*). The expression of *PIN* genes in the *iamt1-1* mutant followed the same transient induction on reorientation as in the wild-type, but with higher transcript levels (*SI Appendix*, Fig. S4 *A* and *B*). More importantly, the increased expression of *PIN* genes in the *iamt1-1* mutant was restored by incubation with NPA at a concentration that rescued gravitropic reorientation (Fig. 3*D* and *SI Appendix*, Fig. S4*C*), indicating that enhanced PAT and increased local accumulation of auxin in the *iamt1* hypocotyls are caused by a perturbance of the auxin-dependent feed-forward loop that promotes auxin transport.

The increase in *PIN3* gene expression in the *iamt1-1* mutant also resulted in higher levels of PIN3 protein, as indicated by the comparably stronger GFP signal in *PIN3::PIN3-GFP* lines throughout the mutant hypocotyls (Fig. 4). Gravistimulation of WT hypocotyls provokes the gradual asymmetrical redistribution of PIN3 to the inner side of endodermal cells in the upper half of hypocotyls (5, 6), being proposed as a major mechanism explaining how the gravity vector is translated into the directional auxin fluxes both in roots and shoots (29). However, we observed that the PIN3-GFP signal in the *iamt1-1* mutant remained in the outer side of endodermal cells even 6 h after gravistimulation (Fig. 4). This explains the mutant defects in both the gravity-mediated asymmetric auxin distribution and hypocotyl bending (Figs. 1*D* and 2 *C* and *D* and *SI Appendix*, Fig. S2*C*). Interestingly, we found that expression of *IAMT1* in the endodermis, but not in the epidermis, was able to rescue the agravitropic phenotype of *iamt1* mutants (Fig. 5 and *SI Appendix*, Fig. S6), indicating that IAA methylation acts locally in the endodermis to establish adequate rates of polar auxin transport. If Me-IAA is simply an inactive form of IAA, methylation could be a fine-tuning mechanism to correct local concentrations of auxin in the tissue that responds to gravity. On the other hand, the possibility that a reduction in auxin methylation can indirectly affect auxin conjugation, or that Me-IAA itself has a direct role as a modulator of auxin signaling or transport, cannot be ruled out. To evaluate this latter possibility, we resorted to orthogonal systems, which allowed the assessment of these processes in a context devoid of other endogenous components that may potentially affect the study. We first reconstructed the IAA perception complex in mammalian cells to observe the event of perception using a ratiometric sensor for auxin (30). Our results showed that Me-IAA neither mimicked the response to IAA in the activity of the auxin coreceptor complex nor interfered with the response triggered by IAA (*SI Appendix*, Fig. S7). Similarly, the presence of intracellular Me-IAA in auxin transport assays using *Xenopus* oocytes (31) reduced PIN1- and PIN3-mediated IAA efflux to the same extent as IAA itself (*SI Appendix*, Fig. S8), suggesting that Me-IAA can be transported by PINs and compete with IAA, and that it is rather unlikely that it acts as an allosteric inhibitor of these transporters.

In summary, we propose that IAA methylation is a biologically relevant mechanism in the endodermis for the maintenance of auxin homeostasis and the appropriate expression levels of *PIN* genes that allow asymmetric auxin distribution under certain circumstances, such as during gravitropic reorientation (Fig. 5*B*). Our results are in line with recent reports highlighting the importance of auxin conjugation in other developmental contexts, such as

Embargoed

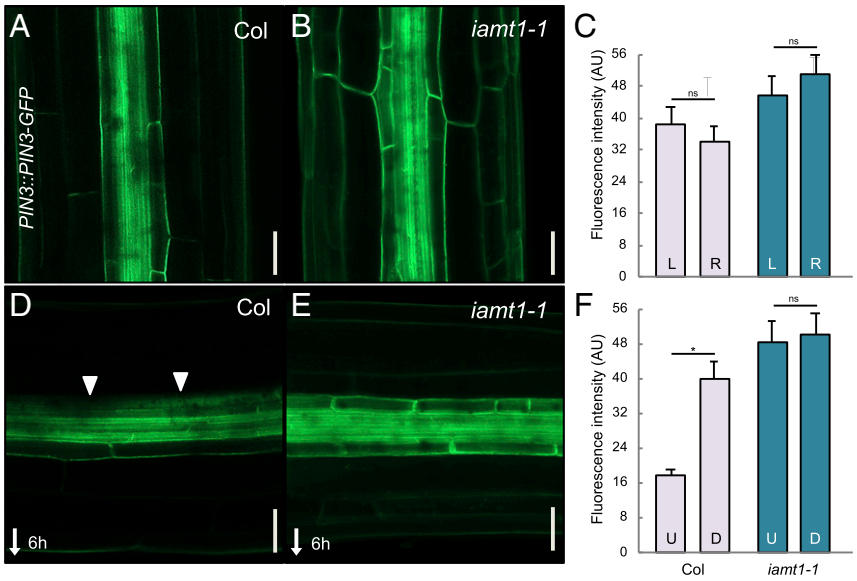


Fig. 4. The *iamt1-1* mutant shows defects in PIN3 lateralization after gravistimulation. (*A* and *B*) Localization of PIN3-GFP in 3-d-old etiolated WT (Col) and *iamt1-1* hypocotyls. (*C*) Quantitative analysis of PIN3-GFP fluorescence in the left and right sections on the hypocotyls. The graph represents the average intensity of fluorescence of the outer and inner endodermal plasma membranes. (*D* and *E*) Localization of PIN3-GFP at 6 h after gravistimulation. (Scale bars: 50 μm.) (*F*) Quantitative analysis of PIN3-GFP in the upper and lower sections on the hypocotyls. Graphs represents the average intensity of fluorescence of endodermal plasma membranes facing away from the vasculature (left and right in vertical hypocotyls; upper and lower in horizontal hypocotyls). Arrows mark the lateralization of PIN3. Error bars represent SD. D, down; L, left; R; right; U, up. The asterisk indicates that the difference is statistically significant (Student's *t* test, $*P < 0.001$).

PNAS proof
Embargoed

shade avoidance and root growth (17, 32). Moreover, the link between auxin transport and the control of an appropriate range of auxin concentrations shown here suggest that both mechanisms have necessarily coevolved to optimize plant adaptation.

Materials and Methods

Plant Material and Growth Conditions. *Arabidopsis thaliana* ecotype Col-0 was used as WT. The following published transgenic and mutant lines were used: *PIN3::PIN3-GFP* (4), *35S::DII-Venus* (33), and *DR5::nGFP* (34). *PIN3::PIN3-GFP*, *DII-Venus*, and *DR5::nGFP* were introgressed into the *iamt1-1* mutant background by crossing. The *iamt1-1* described in this work corresponds to the T-DNA insertion line SALK_072125 (35). This line was genotyped with *IAMT1*-specific oligonucleotides and with an oligonucleotide specific for the T-DNA left border (*SI Appendix*, Table S1). The presence of transgenes in progenies of crosses was determined by the corresponding antibiotic resistance when possible, and also by genotyping (*SI Appendix*, Table S1).

Seeds were sown on 1/2 MS plates with 1% (wt/vol) sucrose and 8 g/L agar, pH 5.8. Seeds were stratified for 3 d at 4 °C, exposed to light for 6–8 h at 20 °C, and then cultivated in the dark. For experiments including chemicals, WT and *iamt1-1* seedlings were grown for 3 d in darkness and then transferred to medium containing 0.125, 0.25, 0.5, 1, and 10 μM NPA (Sigma-Aldrich) for 2 h before rotating the plate 90° for 12 h.

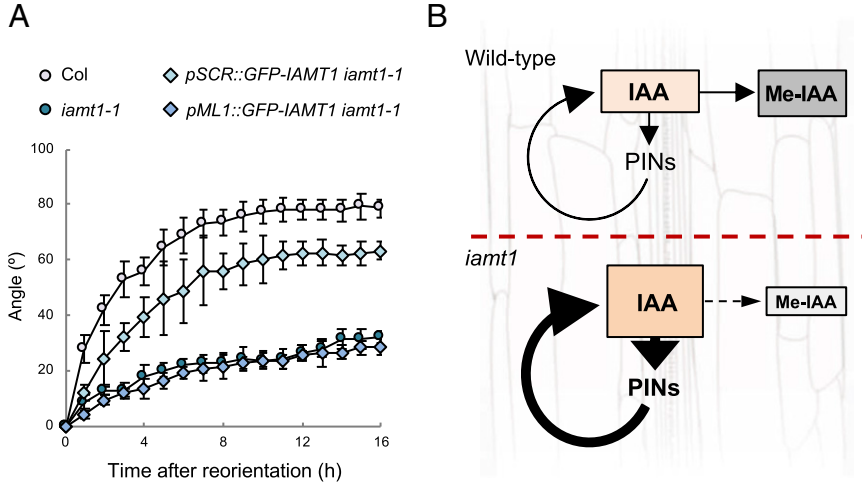


Fig. 5. Auxin methylation in the endodermis is sufficient to ensure gravitropic reorientation. (*A*) Endodermal expression of *IAMT1* is able to recover the *iamt1-1* gravitropic response. Gravitropic reorientation of *iamt1-1* mutant complemented with cell-specific expression of *IAMT1* in endodermis (*pSCR*) and epidermis (*pML1*). The experiments were carried out as described in *Materials and Methods*. Error bars represent SD. (*B*) Model for the role of auxin methylation on gravitropic reorientation. IAMT1 is necessary to maintain relatively low levels of auxin in the responding tissue; in the absence of such mechanism, auxin levels locally increase and enhance the PAT-mediated feedforward loop that causes auxin hyperaccumulation. The relevance of this feedforward loop is highlighted by the rescue of the *iamt1* mutant phenotype by NPA.

In Vivo Plant Imaging. Apical hook development and gravitropic reorientation were monitored as described previously (36, 37). For analysis of the gravity response, 3-d-old etiolated seedlings grown in vertical plates were imaged at 1-h intervals for 16 h after rotating the plate 90°. Hypocotyl angles were measured by ImageJ. Three replicates of at least 10 seedlings with a synchronized germination start were processed.

Confocal Imaging and Signal Quantification. In some cases, hypocotyl cells were visualized by propidium iodide (PI) staining. In these cases, seedlings were rinsed first for 2 min with 10 μg/mL of PI and then for 5 min with water. Fresh stained seedlings were mounted on slides only with water. Images were obtained with a Zeiss 780 Axio Observer confocal microscope for *DR5::nGFP* and with a Zeiss LSM 800 confocal microscope for *DII-Venus* and *PIN3::PIN3-GFP*. For GFP and Venus detection, channel 1 was configured between 500 and 540 nm, and for PI detection, channel 2 was configured between 590 and 660 nm.

Fluorescence intensity was measured in the apical hook and in the bent region of the hypocotyl. The *DII-Venus* and *DR5::nGFP* fluorescence intensity was compared between the inner and outer sides of the apical hook and between the lower and upper sides of the hypocotyl in the responsive part as described previously (6). For quantification of the gravity-induced PIN3-GFP relocation, the PIN3-GFP fluorescence intensity was compared between the outer and inner sides of endodermal cells in both sides of hypocotyls as described previously (6). ImageJ software was used for all intensity measurements. Three replicates of at least 10 seedlings of similar size were processed. Values are presented as the mean of averages. The *t* test was used for statistic evaluation. Error bars in graphs represent SE.

Real-Time Quantitative RT-PCR. Total RNA from 3-d-old etiolated seedlings was extracted using the RNAeasy Plant Mini Kit (Qiagen). cDNA synthesis and quantitative RT-PCR, as well as primer sequences for amplification of *PIN1*, *PIN2*, *PIN3*, *PIN7*, *IAMT1*, and *EF1α* genes, have been described previously (37, 38).

Auxin Transport Assay. For this assay, 3-d-old etiolated seedlings grown on vertical plates containing control medium were transplanted for 6 h to plates with mock or NPA at the indicated concentrations. The upper half of seedlings was placed on top of a small strip of Parafilm M, and a droplet containing 6.75 nM [^{3}H]-IAA (specific activity, 25 Ci/mmol, 1 μCi/μL; Amersham) in 0.1% Tween-20 (Sigma-Aldrich) was applied to cotyledons for 3 h. For auxin transport during gravistimulation, [^{3}H]-IAA was added after seedlings were either allowed to grow straight for another 6 h or plates were rotated 90° for the same time. The lowest 5 mm of the hypocotyl was collected, and radioactivity was measured as described previously (39).

IAA and Me-IAA Quantification. Whole seedlings were immediately frozen in liquid N_2. Approximately 100 mg of tissue was pooled per sample, and at least three biological replicates were harvested for each independent experiment. Then 1 mL of methanol and 50 pmol of [$^2H_2$]-IAA or 100 pmol [$^2H_5$]-Me-IAA were added, the tissue was heated for 2 min at 60 °C, followed by further incubation without heating for at least 1 h. The sample was then taken to complete dryness.

For purification of IAA and Me-IAA, the sediments were dissolved in 2 mL of cold sodium phosphate buffer (50 mM, pH 7.0) containing 5% MeOH, followed by a 10-min ultrasonic treatment (B5510DTH; Branson Ultrasonics). Next, the pH was adjusted to 2.5 with 1 M hydrochloric acid, and the sample was purified by solid-phase extraction using 1 mL/30 mg Oasis HLB columns (Waters) conditioned with 1 mL of methanol and 1 mL of water, and then equilibrated with 0.5 mL of sodium phosphate buffer (acidified with 1 M hydrochloric acid to pH 2.5). After sample application, the column was washed twice with 1 mL of 5% methanol and then eluted with 2 mL of 80% methanol. The elution fraction was taken to complete dryness using a vacuum concentrator (Vacufuge Plus; Eppendorf). After the addition of 20 μL of N,O-bis(trimethylsilyl) trifluoroacetamide containing 1% trimethylchlorosilane (99:1, vol/vol; Supelco) to each extract, the extracts were transferred into 400-μL GC-MS vials and incubated for 70 min at 60 °C.

To analyze IAA and Me-IAA contents in the same samples, 1 μL of each sample was injected splitless with a CombiPAL automated sample injector (CTC Analytics) into a Scion 455 gas chromatograph (Scion Instruments) equipped with a 30 m × 0.25 mm i.d. fused silica capillary column with a chemical bond 0.25-μm ZB35 stationary phase (Phenomenex). Helium at a flow rate of 1 mL/min served as the mobile phase. A pressure pulse of 25 psi over 1 min was used to force the transfer of compounds from the injector into the column. The injector temperature was 250 °C, and the column temperature was held at 50 °C for 1.20 min. Thereafter, the column temperature was increased by 30 °C/min to 120 °C. After reaching 120 °C, the temperature was further increased by 10 °C/min to 325 °C, at which point it was held for another 5 min. The column effluent was introduced into the ion source of a Scion TQ triple-quadruple mass spectrometer. The mass spectrometer was used in EI-MRM mode. The transfer line temperature was set at 250 °C, and the ion source temperature was set at 200 °C. Ions were generated with −70 eV at a filament emission current of 80 μA. The dwell time was 100 ms, and the reactions *m/z* 247 to *m/z* 130 (endogenous IAA), *m/z* 249 to *m/z* 132 ([$^2H_2$]-IAA, internal standard), *m/z* 261 to *m/z* 202 (endogenous Me-IAA), and *m/z* 266 to *m/z* 207 ([$^2H_5$]-Me-IAA, internal standard) were recorded. Argon set at 1.5 mTorr was used as the collision gas. The amount of the endogenous compound was calculated from the signal ratio of the unlabeled over the stable isotope-containing mass fragment observed in the parallel measurements.

Mammalian Cell Culture Orthogonal Platform for Determination of Me-IAA and IAA Signaling with an IAA Sensor. Human embryonic kidney 293-T cells (HEK-293T) were cultivated and transfected as described previously (30). For transfection of each well, 0.55 μg of a plasmid encoding rice TIR1 and 0.2 μg of a plasmid harboring a ratiometric luminescent auxin sensor (with full-length *Arabidopsis* AUX/IAA17 as the sensor module) was mixed and diluted in 50 μL of OptiMEM (Life Technologies) and subsequently mixed with 2.5 μL of PEI solution under vortexing. After 15 min at room temperature, this mixture was added to the cells in a dropwise manner. To induce auxin-mediated protein degradation, appropriate IAA and Me-IAA dilution series were prepared in DMEM and added to the cells at 24 h posttransfection and incubated for 3.5 h, followed by firefly and *Renilla* luminescence analysis as described previously (30).

ACKNOWLEDGMENTS. We thank Cristina Ferrándiz and the members of the Hormone Signaling and Plasticity Laboratory at Instituto de Biología Molecular y Celular de Plantas for discussions and critical reading of the manuscript, and Malcolm Bennett for providing seeds of the reporter lines. Work in the authors' laboratories has been funded by grants from the Spanish Ministry of Economy and Competitiveness (BIO2013-43184-P, to D.A. and M.A.B., and BFU2014-55575-R, to S.P.), the German Research Foundation (EXC-1028-CEPLAS, EXC-294-BIOSS and GSC 4-SGBM, to M.Z.), the European Union (H2020-MSCA-RISE-2014-644435, to M.A.B. and D.A.), and the European Research Council (Project ERC-2011-StG-20101109-PSDP, to J.F.).

1. Vanneste S, Friml J (2009) Auxin: A trigger for change in plant development. *Cell* 136: 1005–1016.
2. Woodward AW, Bartel B (2005) Auxin: Regulation, action, and interaction. *Ann Bot* 95:707–735.
3. Abbas M, Alabadí D, Blázquez MA (2013) Differential growth at the apical hook: All roads lead to auxin. *Front Plant Sci* 4:441.
4. Zádníková P, et al. (2010) Role of PIN-mediated auxin efflux in apical hook development of *Arabidopsis thaliana*. *Development* 137:607–617.
5. Rakusová H, et al. (2016) Termination of shoot gravitropic responses by auxin feedback on PIN3 polarity. *Curr Biol* 26:3026–3032.
6. Rakusová H, et al. (2011) Polarization of PIN3-dependent auxin transport for hypocotyl gravitropic response in *Arabidopsis thaliana*. *Plant J* 67:817–826.
7. Spalding EP (2013) Diverting the downhill flow of auxin to steer growth during tropisms. *Am J Bot* 100:203–214.
8. Muday GK, DeLong A (2001) Polar auxin transport: Controlling where and how much. *Trends Plant Sci* 6:535–542.
9. Swarup R, Bennett M (2003) Auxin transport: The fountain of life in plants? *Dev Cell* 5: 824–826.
10. Adamowski M, Friml J (2015) PIN-dependent auxin transport: Action, regulation, and evolution. *Plant Cell* 27:20–32.
11. Esmon CA, et al. (2006) A gradient of auxin and auxin-dependent transcription precedes tropic growth responses. *Proc Natl Acad Sci USA* 103:236–241.
12. Fuchs I, Philippar K, Ljung K, Sandberg G, Hedrich R (2003) Blue light regulates an auxin-induced K^+-channel gene in the maize coleoptile. *Proc Natl Acad Sci USA* 100: 11795–11800.
13. Hohm T, et al. (2014) Plasma membrane H^+-ATPase regulation is required for auxin gradient formation preceding phototropic growth. *Mol Syst Biol* 10:751.
14. Band LR, et al. (2012) Root gravitropism is regulated by a transient lateral auxin gradient controlled by a tipping-point mechanism. *Proc Natl Acad Sci USA* 109: 4668–4673.
15. Kramer EM (2004) PIN and AUX/LAX proteins: Their role in auxin accumulation. *Trends Plant Sci* 9:578–582.
16. Grieneisen VA, Xu J, Marée AF, Hogeweg P, Scheres B (2007) Auxin transport is sufficient to generate a maximum and gradient guiding root growth. *Nature* 449: 1008–1013.

PNAS proof
Final Article Proof

17. Mellor N, et al. (2016) Dynamic regulation of auxin oxidase and conjugating enzymes AtDAO1 and GH3 modulates auxin homeostasis. *Proc Natl Acad Sci USA* 113: 11022–11027.
18. Porco S, et al. (2016) Dioxygenase-encoding *AtDAO1* gene controls IAA oxidation and homeostasis in *Arabidopsis*. *Proc Natl Acad Sci USA* 113:11016–11021.
19. Zhang J, et al. (2016) DAO1 catalyzes temporal and tissue-specific oxidative inactivation of auxin in *Arabidopsis thaliana*. *Proc Natl Acad Sci USA* 113:11010–11015.
20. Qin G, et al. (2005) An indole-3-acetic acid carboxyl methyltransferase regulates *Arabidopsis* leaf development. *Plant Cell* 17:2693–2704.
21. Zhao N, et al. (2008) Structural, biochemical, and phylogenetic analyses suggest that indole-3-acetic acid methyltransferase is an evolutionarily ancient member of the SABATH family. *Plant Physiol* 146:455–467.
22. Zubieta C, et al. (2003) Structural basis for substrate recognition in the salicylic acid carboxyl methyltransferase family. *Plant Cell* 15:1704–1716.
23. Li L, et al. (2008) The possible action mechanisms of indole-3-acetic acid methyl ester in *Arabidopsis*. *Plant Cell Rep* 27:575–584.
24. Yang Y, et al. (2008) Inactive methyl indole-3-acetic acid ester can be hydrolyzed and activated by several esterases belonging to the AtMES esterase family of *Arabidopsis*. *Plant Physiol* 147:1034–1045.
25. Friml J, Wiśniewska J, Benková E, Mendgen K, Palme K (2002) Lateral relocation of auxin efflux regulator PIN3 mediates tropism in *Arabidopsis*. *Nature* 415:806–809.
26. Péret B, et al. (2013) Sequential induction of auxin efflux and influx carriers regulates lateral root emergence. *Mol Syst Biol* 9:699.
27. Sauer M, et al. (2006) Canalization of auxin flow by Aux/IAA-ARF-dependent feedback regulation of PIN polarity. *Genes Dev* 20:2902–2911.
28. Chen Q, et al. (2015) A coherent transcriptional feed-forward motif model for mediating auxin-sensitive PIN3 expression during lateral root development. *Nat Commun* 6:8821.
29. Rakusová H, Fendrych M, Friml J (2015) Intracellular trafficking and PIN-mediated cell polarity during tropic responses in plants. *Curr Opin Plant Biol* 23:116–123.
30. Wend S, et al. (2013) A quantitative ratiometric sensor for time-resolved analysis of auxin dynamics. *Sci Rep* 3:2052.
31. Zourelidou M, et al. (2014) Auxin efflux by PIN-FORMED proteins is activated by two different protein kinases, D6 PROTEIN KINASE and PINOID. *eLife* 3:02860.
32. Zheng Z, et al. (2016) Local auxin metabolism regulates environment-induced hypocotyl elongation. *Nat Plants* 2:16025.
33. Brunoud G, et al. (2012) A novel sensor to map auxin response and distribution at high spatio-temporal resolution. *Nature* 482:103–106.
34. Friml J, et al. (2003) Efflux-dependent auxin gradients establish the apical-basal axis of *Arabidopsis*. *Nature* 426:147–153.
35. Alonso JM, et al. (2003) Genome-wide insertional mutagenesis of *Arabidopsis thaliana*. *Science* 301:653–657.
36. Abbas M, et al. (2015) Oxygen sensing coordinates photomorphogenesis to facilitate seedling survival. *Curr Biol* 25:1483–1488.
37. Gallego-Bartolomé J, Kami C, Fankhauser C, Alabadí D, Blázquez MA (2011) A hormonal regulatory module that provides flexibility to tropic responses. *Plant Physiol* 156:1819–1825.
38. Frigerio M, et al. (2006) Transcriptional regulation of gibberellin metabolism genes by auxin signaling in *Arabidopsis*. *Plant Physiol* 142:553–563.
39. Willige BC, Isono E, Richter R, Zourelidou M, Schwechheimer C (2011) Gibberellin regulates PIN-FORMED abundance and is required for auxin transport-dependent growth and development in *Arabidopsis thaliana*. *Plant Cell* 23:2184–2195.

PNAS proof
Embargoed

AUTHOR QUERIES

AUTHOR PLEASE ANSWER ALL QUERIES 1

Q: 1_Please contact PNAS_Specialist.djs@sheridan.com if you have questions about the editorial changes, this list of queries, or the figures in your article. Please include your manuscript number in the subject line of all email correspondence; your manuscript number is 201806565.

Q: 2_Please (i) review the author affiliation and footnote symbols carefully, (ii) check the order of the author names, and (iii) check the spelling of all author names, initials, and affiliations. To confirm that the author and affiliation lines are correct, add the comment "OK" next to the author line. This is your final opportunity to correct any errors prior to publication. Misspelled names or missing initials will affect an author's searchability. Once a manuscript publishes online, any corrections (if approved) will require publishing an erratum; there is a processing fee for approved erratum. Please check with your coauthors about how they want their names and affiliations to appear.

Q: 3_Please review the information in the author contribution footnote carefully. Please make sure that the information is correct and that the correct author initials are listed. Note that the order of author initials matches the order of the author line per journal style. You may add contributions to the list in the footnote; however, funding should not be an author's only contribution to the work.

Q: 4_Please note that the spelling of the following author names in the manuscript differs from the spelling provided in the article metadata: Jorge Hernández-García, Matías Zurbriggen, Miguel A. Blázquez, and David Alabadí. The spelling provided in the manuscript has been retained; please confirm.

Q: 5_You have chosen not to pay for the PNAS open access option. Please confirm that this is correct. If this is incorrect, and you would like to pay for the PNAS open access option, please note this in the margin.

Q: 6_Please note that all supporting information (SI) file(s), including the SI Appendix PDF and/or any other files (e.g., datasets, movies), have not been altered in any way and will be posted online as originally submitted. If you have any changes to your SI file(s), please provide new, ready-to-publish replacement files without annotations. If you are unable to view your SI files in the Author Center, or if you have any questions regarding your SI, please contact PNAS_Specialist.djs@sheridan.com.

Q: 7_PNAS allows up to five keywords. You may add one keyword. Also, please check the order of your keywords and approve or reorder them as necessary.

Q: 8_Per PNAS style, certain compound terms are hyphenated when used as adjectives and unhyphenated when used as nouns. This style has been applied consistently throughout where (and if) applicable.

AUTHOR QUERIES

AUTHOR PLEASE ANSWER ALL QUERIES 2

Q: 9_For affiliation "f," please specify the pertinent department/division/section, etc.

Q: 10_PNAS italicizes genes and alleles. All genes, alleles, and proteins will appear as indicated in your proofs. Please carefully check use of italics and capital letters throughout the proof and correct as necessary. If, by "■■■ gene," you mean "the gene that encodes protein ■■■," then italic type is not necessary. (NOTE: If all instances of a gene/allele should be changed, please make only one correction and indicate that it is a global change.)